

$C_a-C_m-C_a = 125.5 (4)^\circ$ ,  $N-C_a-C_b = 108.4 (3)^\circ$ , and  $C_a-C_b-C_b = 107.8 (4)^\circ$ . The range of values for any chemical class is satisfyingly small.

**Acknowledgment.** The support of this work by the National Institutes of Health (Grant HL-15627) is gratefully acknowledged. We thank Prof. W. G. Woodruff for a preprint and a useful

discussion.

**Registry No.** [Fe(TPP)(F)<sub>2</sub>][2-MeHIm]·2CHCl<sub>3</sub>, 84238-03-9.

**Supplementary Material Available:** Table II (anisotropic temperature factors), Table IV (fixed hydrogen atom positions), and a listing of the structure factor amplitudes (X10) (19 pages). Ordering information is given on any current masthead page.

## Proton NMR Characterization of the Ferryl Group in Model Heme Complexes and Hemoproteins: Evidence for the Fe<sup>IV</sup>=O Group in Ferryl Myoglobin and Compound II of Horseradish Peroxidase

Gerd N. La Mar,\* Jeffrey S. de Ropp, Lechoslaw Latos-Grazynski, Alan L. Balch,\* R. B. Johnson, Kevin M. Smith, Daniel W. Parish, and Ru-Jen Cheng

Contribution from the Department of Chemistry, University of California, Davis, California 95616. Received March 23, 1982

**Abstract:** The proton NMR spectra of model porphyrin complexes possessing the ferryl, Fe<sup>IV</sup>=O, group are reported and assigned. The only resonance shifted well outside the diamagnetic region is that of the meso protons. Moreover, these model compounds exhibit hyperfine shift patterns (particularly for the substituents found in natural porphyrins) that are different from those found for other characterized iron-porphyrin complexes. Deuterium labeling of the meso position of hemin reconstituted into sperm whale myoglobin and horseradish peroxidase reveals that both the hydrogen peroxide treated myoglobin (ferryl myoglobin) and horseradish peroxidase compound II exhibit only meso H resonances with significant hyperfine shift and that these shifts are essentially the same as those found in the low-spin Fe<sup>IV</sup>=O model complexes. Hence, the <sup>1</sup>H NMR data can be taken as evidence for the presence of the ferryl group at the active site of both ferryl myoglobin and compound II of horseradish peroxidase.

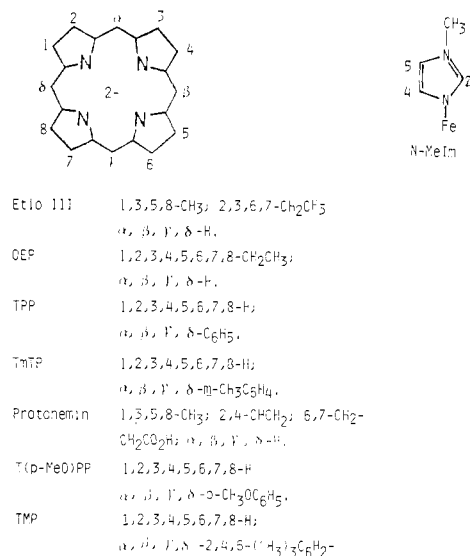
The ferryl unit (Fe<sup>IV</sup>=O) has been proposed to describe the heme iron in the reactive intermediates of horseradish peroxidase, HRP, chloroperoxidase, CP, as well as the reaction product of hydrogen peroxide with myoglobin, ferryl Mb.<sup>1-13</sup> Evidence for the presence of a low-spin ( $S = 1$ ) iron(IV) includes magnetic susceptibility<sup>14</sup> and Mössbauer data of horseradish peroxidase compound II (HRP-II).<sup>15-17</sup> The presence of an oxo ligand has

been confirmed by chemical reactivity for compound I of chloroperoxidase (CP-I)<sup>1</sup> and on the basis of <sup>17</sup>O hyperfine structure in the ESR spectrum of compound I of horseradish peroxidase, HRP-I.<sup>18</sup> In the latter case, the absence of proton hyperfine splittings has been used to argue directly for the Fe<sup>IV</sup>=O unit, with the second oxidizing equivalent residing on the porphyrin. The presence of an oxo ligand in proteins one oxidizing equivalent above the resting ferric state, HRP-II and ferryl Mb,<sup>12,13</sup> is not as well documented.

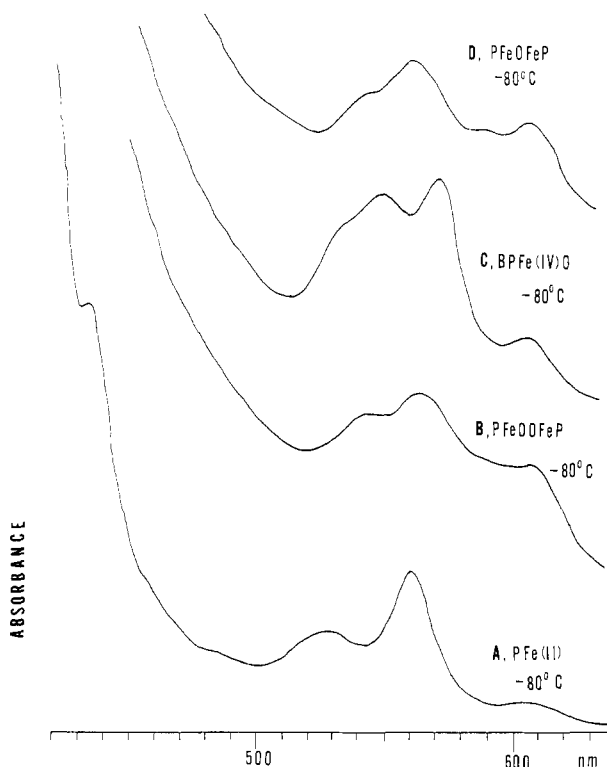
<sup>1</sup>H NMR spectroscopy of paramagnetic hemoprotein provides a particularly useful tool for characterizing the oxidation/spin/ligation states of the iron.<sup>19-22</sup> The largely scalar interaction with the unpaired spin(s) at the metal induces large hyperfine shifts for the heme substituent protons which not only permit resolution of many of the resonances in regions outside the crowded diamagnetic envelope but also allow assignment of electronic structure

- (1) Hager, L. P.; Doubek, D. L.; Silverstein, R. M.; Hargis, J. H.; Martin, J. C. *J. Am. Chem. Soc.* **1972**, *94*, 4364-4366.
- (2) Dunford, H. B.; Stillman, J. S. *Coord. Chem. Rev.* **1976**, *19*, 187-251.
- (3) Yamazaki, I.; Arais, T.; Hayashi, Y.; Yamada, H.; Makino, R. *Adv. Biophys.* **1978**, *11*, 249-281.
- (4) Yamazaki, I.; Yokota, K. *Mol. Cell. Biochem.* **1973**, *2*, 39-52.
- (5) Hansen, L. K.; Chang, C. K.; Davis, M. S.; Fajer, J. *J. Am. Chem. Soc.* **1981**, *103*, 663-670.
- (6) Loew, G. H.; Kert, C. J.; Hjelmeland, L. M.; Kirchner, R. F. *J. Am. Chem. Soc.* **1977**, *99*, 3534-3535.
- (7) Schonbaum, G. R.; Chance, B. *Enzymes 3rd Ed.* **1976**, *13*, 363-408.
- (8) Fox, J. B., Jr.; Nicholas, R. A.; Ackerman, S. A.; Swift, C. E. *Biochemistry* **1974**, *13*, 5178-5186.
- (9) Aasa, R.; Vannngord, T. M.; Dunford, H. B. *Biochim. Biophys. Acta.* **1975**, *391*, 259-264.
- (10) McIntosh, A. R.; Stillman, M. J. *Biochem. J.* **1977**, *167*, 31-37.
- (11) Chu, M.; Dunford, H. B.; Job, D. *Biochem. Biophys. Res. Commun.* **1977**, *74*, 159-164.
- (12) King, N. K.; Windfield, M. E. *J. Biol. Chem.* **1963**, *238*, 1520-1528.
- (13) Uyeda, M.; Peisach, J. *Biochemistry* **1981**, *20*, 2028-2035.
- (14) Theorell, M.; Ehrenberg, A. *Arch. Biochem. Biophys.* **1952**, *41*, 442-461.
- (15) Maeda, Y.; Morita, Y. *Biochem. Biophys. Res. Commun.* **1967**, *29*, 680-685.

- (16) Moss, T. H.; Ehrenberg, A.; Boniden, A. *J. Biochemistry* **1969**, *8*, 4159-4162.
- (17) Schulz, C. E.; Devaney, P. W.; Wintker, M.; Debrunner, P. G.; Doan, N.; Chiang, R.; Rutter, R.; Hager, L. P. *FEBS Lett.* **1979**, *103*, 102-105.
- (18) Roberts, J. E.; Hoffman, B.; Rutter, R.; Hager, L. P. *J. Am. Chem. Soc.* **1981**, *103*, 7654-7656.
- (19) La Mar, G. N. In "Biological Applications of Magnetic Resonance"; Schulman, R. G., Ed.; Academic Press: New York, 1979; pp 305-343.
- (20) La Mar, G. N.; de Ropp, J. S.; Smith, K. M.; Langry, K. C. *J. Biol. Chem.* **1980**, *255*, 6646-6652.
- (21) La Mar, G. N.; de Ropp, J. S.; Smith, K. M.; Langry, K. C. *J. Biol. Chem.* **1981**, *256*, 237-243.
- (22) Latos-Grazynski, L.; Balch, A. L.; La Mar, G. N. In "Electrochemical and Spectrochemical Studies of Biological Redox Components"; Kadish, K. M.; Ed.; ACS Advances in Chemistry, **1982**, *201*, 661-674.

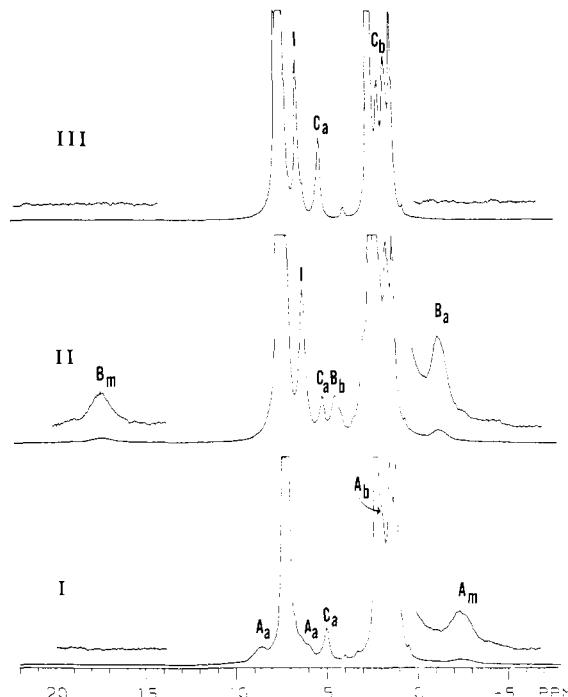


**Figure 1.** Labeling schemes for porphyrin derivatives and *N*-methylimidazole.



**Figure 2.** Optical spectra of (Etio)PFe(II) in toluene solution at  $-80^{\circ}\text{C}$ . Trace A, (Etio)PFe(II); trace B, (Etio)PFe(II), with dioxxygen added, (Etio)FeOFe(Etio) is present; trace C, the same sample after the addition of *N*-Melm, (*N*-Melm)(Etio)FeO is present; trace D, this sample after warming to  $25^{\circ}\text{C}$  and cooling to  $-80^{\circ}\text{C}$ , (Etio)FeOFe(Etio) is present.

based on characteristic hyperfine shift patterns for various heme functional groups.<sup>23</sup> The assignment of electronic structure is based on the observation that the hyperfine shift pattern for the protoporphyrin substituents is distinct for each previously characterized oxidation/spin/ligation state of heme iron, and that the pattern is essentially the same in model compounds and intact hemoproteins possessing the same molecular and electronic structure.<sup>22,24</sup> Meaningful comparison of the  $^1\text{H}$  NMR spectra



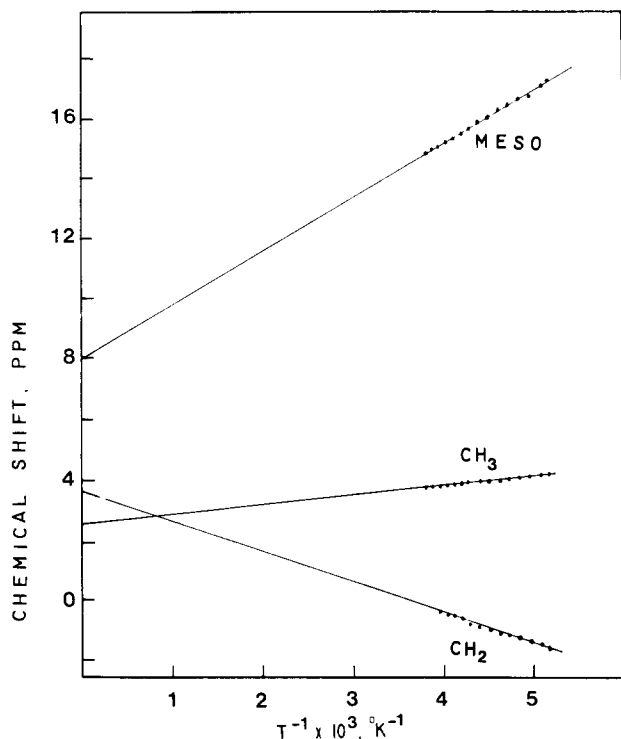


**Figure 4.** Curie plot of the resonances of  $(N\text{-MeIm})(\text{Etio})\text{Fe}^{\text{IV}}=\text{O}$ . Resonances due to the porphyrin-bound methyl groups and the axial ligand are not observed.

$(\text{Etio})\text{FeOFe}(\text{Etio})$ , as seen in trace D.

Corresponding  $^1\text{H}$  NMR spectra are shown in Figure 3. Trace I shows the spectrum of  $(\text{Etio})\text{Fe}(\text{II})$  after the admission of dioxygen at  $-70^\circ\text{C}$ . Peaks of the compound, identified as  $(\text{Etio})\text{FeOOFe}(\text{Etio})$ , are assigned by comparison with the spectra of  $(\text{OEP})\text{FeOFe}(\text{OEP})$  and of  $(\text{OEP})\text{FeOOFe}(\text{OEP})$ .<sup>30</sup> Based on meso deuteration of the corresponding OEP compound, the broadest resonance (at  $-2.5$  ppm) is assigned to the meso protons. This resonance shows clear evidence of the antiferromagnetic character since it shifts 0.5 ppm upfield on increasing the temperature from  $-75$  to  $-20^\circ\text{C}$ . The spectra of  $(\text{Etio})\text{FeOOFe}(\text{Etio})$  and  $(\text{OEP})\text{FeOOFe}(\text{OEP})$  show larger spreads of hyperfine shifts than either  $(\text{OEP})\text{FeOFe}(\text{OEP})$  or  $(\text{Etio})\text{FeOFe}(\text{Etio})$ . This is predicted if the antiferromagnetic coupling in the peroxo-bridged species is weaker than that in the oxo-bridged counterparts as found in the peroxo-bridged dimers already characterized.<sup>27</sup>

On addition of excess  $N\text{-MeIm}$  to  $(\text{Etio})\text{FeOOFe}(\text{Etio})$ , the resonances of the peroxo-bridged dimer vanish and resonances of a new intermediate shown in trace II of Figure 3 appear. This intermediate is thermally unstable and is converted to  $(\text{Etio})\text{-FeOFe}(\text{Etio})$  on warming as seen in trace III of Figure 3. The  $^1\text{H}$  NMR resonances of  $(N\text{-MeIm})(\text{Etio})\text{FeO}$  shown in Figure 3 have been assigned on the basis of their relative intensities and their extrapolated positions at infinite temperature. A Curie plot for this species is shown in Figure 4. The resonances obey the Curie law and extrapolate to the appropriate regions of the diamagnetic spectrum. The unique strict obedience to the Curie law

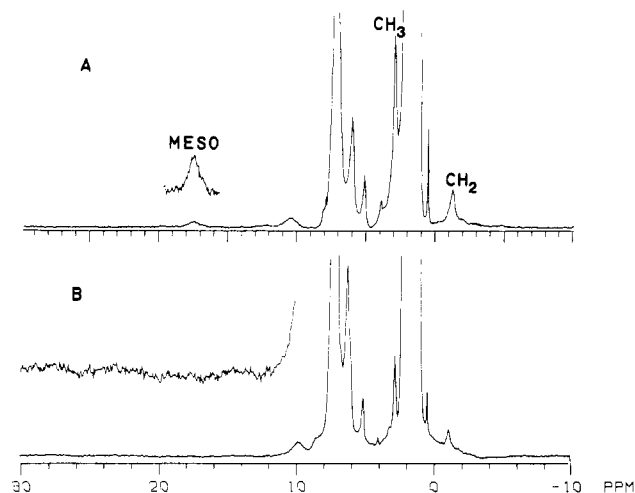


**Figure 5.**  $^1\text{H}$  NMR spectra at 360 MHz of: A,  $(N\text{-MeIm})(\text{OEP})\text{FeO}$  at  $-80^\circ\text{C}$ , labeled peaks give the resonance assignment of peaks due to the thermally unstable intermediate; B,  $(N\text{-MeIm})(\text{OEP-}m\text{-}d_4)\text{FeO}$  at  $-70^\circ\text{C}$ . Peaks due to the solvent (toluene- $d_7$ ) have been cut off. The peak at 6.5 ppm is due to excess  $N\text{-MeIm}$ , other peaks arise from iron(III) porphyrins.

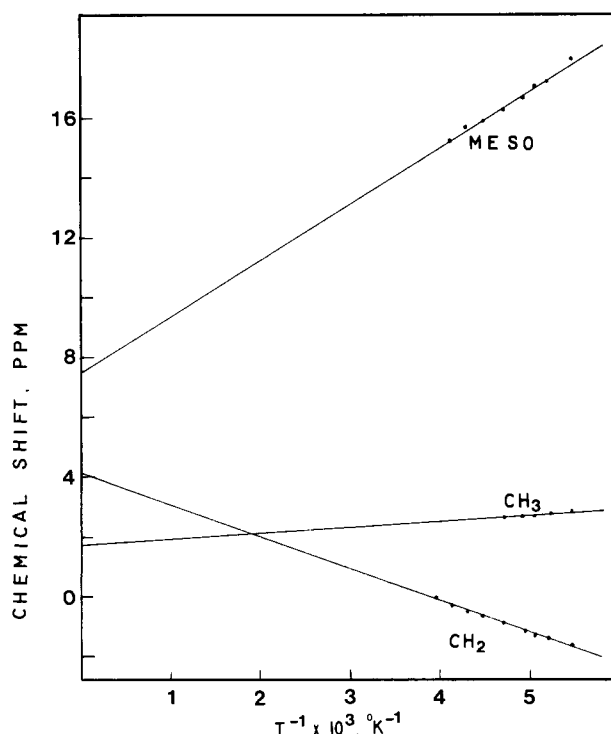


**Figure 6.** Curie plot of the resonances of  $(N\text{-MeIm})(\text{OEP})\text{Fe}^{\text{IV}}=\text{O}$ .

has been previously found for the corresponding  $(N\text{-MeIm})\text{-}(\text{TPP})\text{FeO}$ .<sup>25</sup>

Addition of  $N\text{-MeIm}$  to  $(\text{OEP})\text{FeOOFe}(\text{OEP})$  yields a similar species,  $(N\text{-MeIm})(\text{OEP})\text{FeO}$ . Its  $^1\text{H}$  NMR spectrum is shown in Figure 5 along with the spectrum of meso-deuterated species,  $(N\text{-MeIm})(\text{OEP-}m\text{-}d_4)\text{FeO}$ . Comparison of these spectra allows for the unambiguous assignment of the resonance of the meso protons of the porphyrin. A Curie plot for this species is given in Figure 6.

The hyperfine-shifted regions of the 360-MHz proton NMR spectra of sperm whale ferryl Mb and HRP-II at  $25^\circ\text{C}$  in  $^2\text{H}_2\text{O}$  are illustrated in the lower traces of Figures 7 and 8, respectively. The spectra are the same as those reported previously<sup>31-33</sup> except

(28) O'Keefe, D. H.; Barlow, C. H.; Smythe, G. A.; Fuchsman, W. H.; Moss, T. H.; Lilienthal, H. R.; Caughey, W. S. *Bioinorg. Chem.* **1975**, *5*, 125-147.

(29) La Mar, G. N.; Eaton, G. R.; Holm, R. M.; Walker, F. A. *J. Am. Chem. Soc.* **1973**, *95*, 63-75.

(30) Previously we reported<sup>27</sup> that no  $^1\text{H}$  NMR spectrum could be recorded at 100 MHz for  $(\text{OEP})\text{FeOOFe}(\text{OEP})$  and speculated that the resonances of this species lay near the diamagnetic region and possibly were obscured by solvent resonances. Utilizing the enhanced sensitivity available at 360 MHz, we find the following resonances  $(\text{OEP})\text{FeOOFe}(\text{OEP})$  at  $-75^\circ\text{C}$ : meso protons,  $-2.33$  ppm confirmed by selective deuteration; 8.85, 6.26, methylene protons; 1.74 ppm, methyl protons. The pattern of resonance shifts and relative line widths are similar to those of  $(\text{OEP})\text{FeOFe}(\text{OEP})$  but the peroxo-bridged dimer has, as expected, larger hyperfine shifts.

(31) Morishima, I.; Ogawa, S. *J. Am. Chem. Soc.* **1978**, *100*, 7125-7127.

(32) Morishima, I.; Ogawa, S. *Biochem. Biophys. Res. Commun.* **1978**, *83*, 946-953.

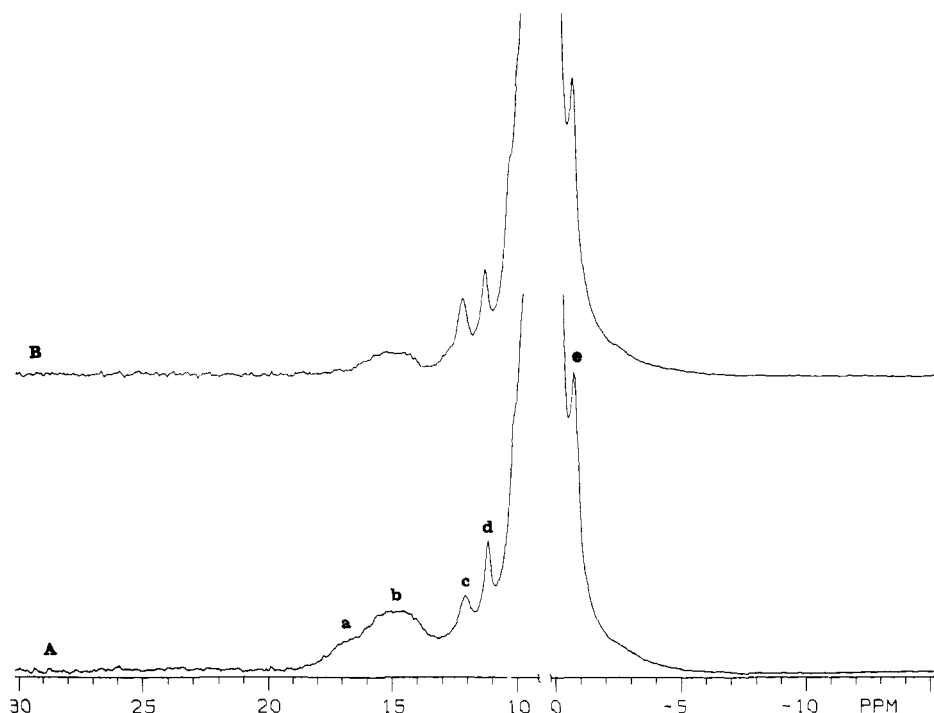


**Figure 7.** Hyperfine shifted regions of the 360-MHz  $^1\text{H}$  spectra of (A) sperm whale ferryl Mb and (B) sperm whale ferryl [ $\text{meso-}^2\text{H}_4$ ]Mb. Proteins in 0.2 M NaCl 99.8%  $^2\text{H}_2\text{O}$  at pH 7.8, 25  $^\circ\text{C}$ . The upfield portions of the spectra (shifts greater than 0 ppm) are plotted at  $1/4$  the vertical scale of the downfield portions.

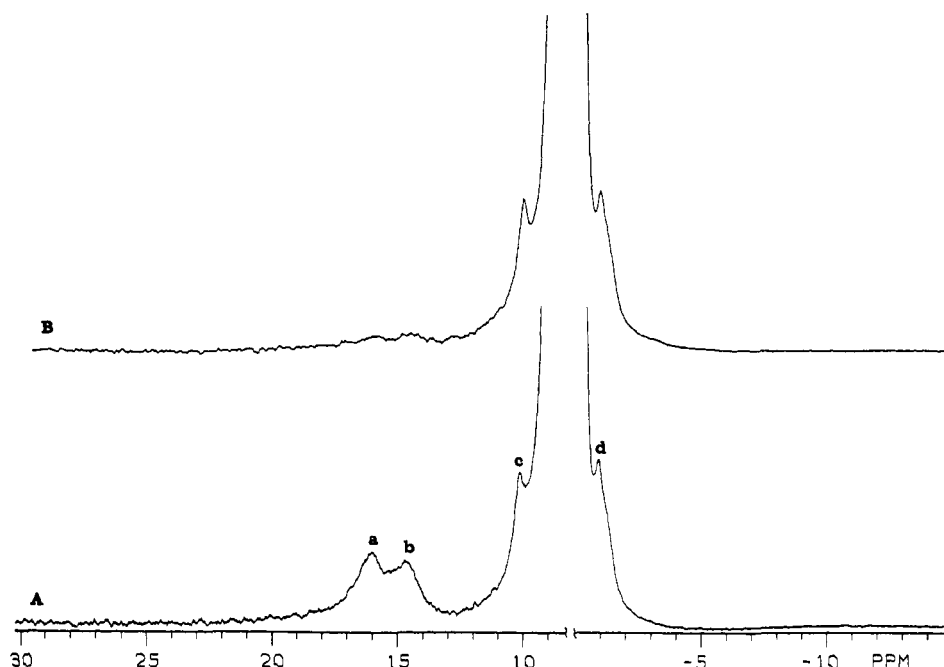


**Figure 8.** Hyperfine shifted regions of the 360-MHz  $^1\text{H}$  spectra of (A) HRP-II and (B) [ $\text{meso-}^2\text{H}_4$ ]HRP-II in 0.2 M NaCl 99.8%  $^2\text{H}_2\text{O}$  at pH 9.2, 25  $^\circ\text{C}$ . The upfield portions of the spectra (shifts greater than 0 ppm) are plotted at  $1/4$  the vertical scale of the downfield portions.

for the improved resolution and sensitivity. The  $^1\text{H}$  NMR spectra of horse and sperm whale ferryl Mb are essentially identical. Proton NMR spectra under identical conditions for ferryl Mb and HRP-II, each reconstituted with hemin deuterated at the meso position, are found in the upper part of Figures 7 and 8. The intensities of the resonances in the region 14–16 ppm for each protein are significantly affected by the deuteration.

#### Discussion

**Model Compounds.** The  $^1\text{H}$  NMR spectra of the reaction products at  $-80\text{ }^\circ\text{C}$  of the reduced  $\text{PFe}^{\text{II}}$  (P = OEP, Etio) with

dioxygen are indicative of antiferromagnetic  $\text{PFeOOFeP}$  dimers with larger hyperfine shifts but the same shift pattern as found for the better known  $\mu$ -oxo dimer analogues. These peroxo-bridged compounds, as expected, decompose to the  $\mu$ -oxo dimers upon raising the temperature. However, the peroxo dimers of OEP and Etio, as found previously for the TPP complex, react with *N*-MeIm at  $-80\text{ }^\circ\text{C}$  to yield new species, which we have shown earlier to be a low-spin iron(IV) complex (B) $\text{PFe}^{\text{IV}}=\text{O}$ .<sup>25,26</sup> The NMR spectra are shown in Figures 3 and 5. The Curie plots for both compounds are strictly linear (Figure 4), as also demonstrated for (B)(TPP) $\text{Fe}^{\text{IV}}=\text{O}$ . The downfield resonance for OEP is clearly assigned to the meso protons upon comparison of the spectra for (B) $\text{PFe}^{\text{IV}}=\text{O}$  with P = OEP and [ $\text{meso-}^2\text{H}_4$ ]OEP in Figure 5.

Table I. Magnetic Properties of Highly Oxidized Iron Porphyrins

compd	$\mu_{\text{eff}}$ , $\mu_B$	$^1\text{H}$ chemical shifts, ppm							$T$ , K	ref
		pyrr <sup>b</sup> H	meso H	pyrr <sup>b</sup> CH <sub>2</sub>	pyrr <sup>b</sup> CH <sub>3</sub>	<i>o</i> -Ph	<i>m</i> -Ph	<i>p</i> -Ph		
( <i>N</i> -MeIm)(TPP)FeO	2.9	5				9	8	8	200	25
( <i>N</i> -MeIm)(OEP)FeO			15	-1					222	this work
( <i>N</i> -MeIm)(Etio)FeO			16	-1	4				222	this work
( <i>T</i> ( <i>p</i> -MeO)PP)FeCl(ClO <sub>4</sub> )	5.1	73				65	-15	-10 <sup>a</sup>	235	34-36
(OEP)FeCl(ClO <sub>4</sub> )			-40	40					223	37
(Etio)FeCl(ClO <sub>4</sub> )			-40	43	62				222	37
( <i>T</i> ( <i>p</i> -MeO)PP)Fe( <i>N</i> -MeIm) <sub>2</sub> Cl(ClO <sub>4</sub> )	2.8	-41				-33	24	13 <sup>a</sup>	235	37
(OEP)Fe( <i>N</i> -MeIm) <sub>2</sub> Cl(ClO <sub>4</sub> )	~3.3			+52					223	37
(Etio)Fe( <i>N</i> -MeIm) <sub>2</sub> Cl(ClO <sub>4</sub> )				50	133				222	37
(TMP)FeCl + PhIO	2.9	-33.5				2.4 <sup>a</sup>	7.6	2.8 <sup>a</sup>	225	38
(TMP)FeCl + <i>m</i> -ClC <sub>6</sub> H <sub>4</sub> CO <sub>3</sub> H	4.2	-27				26.24 <sup>a</sup>	68	11.1 <sup>a</sup>	221	38

<sup>a</sup> Methyl resonances. <sup>b</sup> Pyrrole = pyrr.

The pyrrole substituent resonances are assigned on the basis of intensities and the extrapolated diamagnetic intercept in Figure 4, which in each case correspond to the chemical shift for the functional group in a diamagnetic porphyrin complex. Although (B)(Etio)Fe<sup>IV</sup>=O possesses no rotational symmetry, the hyperfine shifts for the four meso or pyrrole substituents occur as single, unresolved peaks. The shifts extrapolated to 25 °C are meso H, 14 ppm; pyrr  $\alpha$ -CH<sub>2</sub>, 0.5 ppm; pyrr  $\beta$ -CH<sub>3</sub>, 3.5 ppm; and pyrr  $\alpha$ -CH<sub>3</sub>, 1.0 ppm, relative to Me<sub>4</sub>Si.

The extremely small hyperfine shifts relative to other paramagnetic iron porphyrins exhibited by the various ferryl porphyrin substituents is indicative of a high degree of localization of the unpaired spin density on the iron and/or oxygen. Charge iterative extended Hückel calculations on such a compound have, in fact, predicted that the two unpaired spins are shared approximately equally by the Fe and O with negligible participation by porphyrin orbitals.<sup>5</sup>

Comparison of the hyperfine shift pattern for the (*N*-MeIm)PFeO complexes with those of all characterized ferric and ferrous species reveals that they are distinct and outside the range exhibited by the more common oxidation states. A table of relevant  $^1\text{H}$  NMR data for complexes of iron(II) and iron(III) is available.<sup>24</sup> Table I summarizes the available data for more highly oxidized iron porphyrins.<sup>34-38</sup> The shifts for (*N*-MeIm)PFeO are considerably smaller and different in pattern from complexes of the type PFeCl(ClO<sub>4</sub>). These latter complexes were originally formulated as high-spin iron(IV) species, but more recently, evidence for an iron(III)-porphyrin  $\pi$  cation radical formulation has been presented.<sup>39-41</sup> Base adducts of these species, PFe(*N*-MeIm)<sub>2</sub>Cl(ClO<sub>4</sub>), which appear to be low-spin iron(III) complexes of porphyrin  $\pi$  cation radicals, exhibit large upfield shifts for the pyrrole protons as well as large meso phenyl shifts.<sup>37</sup> Likewise the unusually reactive intermediates formed by treating iron(III)-porphyrin chlorides with oxygen donors, iodosylbenzene or 3-chloroperbenzoic acid, show large pyrrole shifts.<sup>38</sup> Thus the present hyperfine shift pattern may reflect the characteristic stabilization by the oxo ligand of a true iron-centered tetravalent oxidation state. For the purpose of elucidating the electron structure of hemoproteins possessing the ferryl group, it is obvious that only the meso H can be expected to be directly resolvable outside the crowded diamagnetic region 0-10 ppm.<sup>42</sup>

**Proteins.** The proton NMR spectrum of sperm whale ferryl Mb exhibits three hyperfine shifted resonances on the low-field side of the diamagnetic envelope, peaks a, b, and c in Figure 7. Integration on the ill-defined base line indicates equal intensities for peaks a and b, with each approximately twice the area of peak c. A shoulder, d, is observed on the high-field side. The earlier report attributed peaks a and b to two of the four heme methyls.<sup>32</sup> Comparison of the upper and lower traces in Figure 7, however, clearly demonstrates that peaks a and b are both reduced in intensity by approximately 80%, which is the degree of deuteration of exclusively the meso position. Hence, peaks a and b must arise each from a pair of unresolved meso H's. Peaks c and d probably arise from amino acid residues.

Previous proton NMR studies of HRP-II at 220 MHz reported two peaks in the region 15 ppm which exhibited Curie behavior and reflected the presence of a tritatable protein residue with  $pK \sim 5.6$ .<sup>32</sup> At 360 MHz, we see a composite resonance at 14.8 ppm, b, with a low-field shoulder, a, and two resolved peaks, c and d below 10 ppm, as shown in A of Figure 8. If peaks c and d represent single protons, the area under peaks a and b is estimated to be 3-6 protons. A single resolved multiproton resonance, e, is observed on the high-field side.

Comparison of the trace of HRP-II with that of HRP-II reconstituted with *meso*-<sup>2</sup>H<sub>4</sub>-hemin (Figure 8) again shows that the low-field peaks are decreased in intensity. The shoulder, a, is not detectable and the major component, b, is reduced in intensity by over a factor of 4. Thus the meso deuteration establishes that peaks a and b also arise from meso H's, with a probably representing a single proton and b resulting from the remaining three meso H's. The much smaller line width for peaks c and d suggest an amino acid origin.

Thus, the characteristic  $^1\text{H}$  NMR spectral features of ferryl Mb and HRP-II are hyperfine shifted resonances in essentially the same spectral window, 14-16 ppm. These arise from the same functional group, the four meso H's. Moreover, this spectral feature and the absence of other hyperfine shifted signals outside the 0-10 ppm region are identical with those found for the low-spin iron(IV)-oxo porphyrins possessing axial imidazoles and are distinct from those exhibited by other ligation and spin states of hemoproteins and model compounds. Hence, we interpret our NMR data as direct evidence for an iron(IV)-oxo(ferryl group) in H<sub>2</sub>O<sub>2</sub>-treated Mb and HRP-II. A similar and complementary

(34) Felton, R. H.; Owen, G. S.; Dolphin, D.; Forman, A.; Borg, D. C.; Fajer, J. *Ann. N.Y. Acad. Sci.* **1972**, *206*, 504-514.

(35) Philippi, M. A.; Goff, H. M. *J. Am. Chem. Soc.* **1979**, *101*, 7641-7643.

(36) Philippi, M. A.; Goff, H. M. *J. Am. Chem. Soc.* **1982**, *104*, 6026.

(37) Goff, H. M., private communication.

(38) Groves, J. T.; Haushalter, R. C.; Nakamura, M.; Nemo, T. E.; Evans, B. J. *J. Am. Chem. Soc.* **1981**, *103*, 2884-2886.

(39) Gaus, P.; Marchen, J. C.; Reed, C. A.; Regnard, J. R. *Nouv. J. Chim.* **1981**, *5*, 203-204.

(40) Philippi, M. A.; Shimomura, E. T.; Goff, H. M. *Inorg. Chem.* **1981**, *20*, 1322-1325.

(41) Shimomura, E. T.; Philippi, M. A.; Goff, H. M.; Scholz, W. F.; Reed, C. A. *J. Am. Chem. Soc.* **1981**, *103*, 6778-6780.

(42) It has been possible to identify a resonance due the axial ligand, *N*-MeIm, by observing the  $^1\text{H}$  NMR spectrum of the very soluble (*N*-MeIm)(TmTP)FeO. A resonance at -4 ppm (line width 350 MHz) with integrated intensity equivalent to one proton per heme is observed in the spectrum of (*N*-MeIm)TmTPFeO in toluene-*d*<sub>6</sub> solution at -80 °C. The intensity and line width of this resonance argue for its assignment to the 5-H proton of *N*-MeIm. The resonances of the other two protons of the axial *N*-MeIm are predicted to be broadened beyond detectability. In the proteins this 5-H proton is replaced by a methylene group whose hyperfine shift is expected to be much smaller and hence resonate within the diamagnetic region 0-10 ppm.

(43) Simmonneaux, G.; Scholz, W. F.; Reed, C. A.; Lang, G. *Biochim. Biophys. Acta* **1982**, *716*, 1-7.

conclusion has been reached on the basis of comparison of the Mössbauer spectrum of (*N*-MeIm)TPPFe<sup>IV</sup>O with those of HRP-II and compound ES of cytochrome *c* peroxidase.<sup>41</sup>

The presence of a coordinated oxygen in HRP-II could have been inferred from the <sup>17</sup>O hyperfine in the ESR spectrum of HRP-I as well as isotope labeling studies of CP-I.<sup>18</sup> Our NMR data support this inference and moreover indicate that it is in the oxo form. The coordinated oxygen is unlikely to be protonated, inasmuch as protonation should characteristically affect the oxygen's ability to stabilize the iron(IV) and localize the spin density in the Fe-O bond and hence should lead to a significantly altered hyperfine shift pattern for the heme resonances. The sensitivity of the hyperfine shifts of iron porphyrins to protonation can be seen in the differences in the <sup>1</sup>H NMR spectra reported for the red and green intermediates formed by the addition of iodosylbenzene or acids to (TMP)FeCl.<sup>38</sup> These intermediates, which are interconverted by acid/base reactions, are more highly oxidized than (*N*-MeIm)PFeO and are, therefore, not directly relevant to the electronic structure of HRP-II itself. This support for Fe<sup>IV</sup>=O in HRP-II poses somewhat of a dilemma since the absence of an exchangeable proton ENDOR signal in HRP-I has also been interpreted in terms of a Fe<sup>IV</sup>=O unit, and it is known that reduction of HRP-I to HRP-II involves the addition of both an electron and a proton.<sup>3</sup> It has been tacitly assumed that this proton is added to the coordinated oxygen. The combination of the recent ENDOR and the present NMR data suggests that this proton may, in fact, be added to a nearby protein residue.

### Experimental Section

**Materials.** Etioporphyrin III<sup>44</sup> and *meso*-tetra-deutero-octaethylporphyrin<sup>45</sup> were prepared as reported previously. Other porphyrins were obtained commercially. Protoporphyrin IX dimethyl ester was deuterated at the meso positions by using a modification of the hexapyridyl-magnesium diiodide method.<sup>45,46</sup> Thus, hexapyridylmagnesium diiodide was prepared by heating a mixture of magnesium turnings (800 mg) and iodine (1.5 g) in anhydrous ether (30 mL) until the iodine color had been dispelled (80 min). The resulting pale yellow solution was filtered to remove excess magnesium and then evaporated to give a yellow solid which was quenched in dry pyridine (50 mL). To this was added CH<sub>3</sub>O<sup>2</sup>H (8 mL) and the golden colored solution was treated with protoporphyrin IX dimethyl ester (300 mg). The resulting mixture was heated under reflux in a dry nitrogen atmosphere for 64 h. After cooling and dilution with methylene chloride (50 mL), the mixture was washed with 2 N hydrochloric acid and then with water and dried (Na<sub>2</sub>SO<sub>4</sub>). Evaporation to dryness gave a red residue which was chromatographed on an alumina column (Brockmann Grade III, elution with methylene chloride). Evaporation of the red eluates gave a purple solid which was crystallized from methylene chloride/hexane to give 65 mg (22% recovery) of protoporphyrin IX dimethyl ester. Iron insertion and hydrolysis<sup>47</sup> gave a sample of protohemin which was shown by NMR spectroscopy to be approximately 80% deuterated at the meso positions and less than 50% at the vinyl β-CH<sub>2</sub>.

**Preparation of Samples of (B)PFe<sup>IV</sup>=O.** Unligated iron(II) porphyrins were prepared by reduction of the appropriate iron(II) complex in toluene solution with an aqueous sodium dithionite solution<sup>48,49</sup> in a Kiwanee controlled-atmosphere box under purified nitrogen. Typically

1 mg of iron(III) porphyrin and 5 mg of sodium dithionite were dissolved in a mixture of 0.5 mL of toluene and several drops of water. The solutions were shaken to mix the two layers. After reduction was complete, as noted by a color change from green-brown to red, the two layers were allowed to separate. The aqueous layer was removed by a pipet. The toluene solution was then washed with a fresh sample of deoxygenated water to remove any remaining inorganic salts. The toluene was evaporated from the sample under vacuum and the sample was dried for 12 h under continuous vacuum. The iron-porphyrin was then dissolved in deoxygenated toluene-*d*<sub>7</sub> and transferred into an NMR tube or cuvette in the controlled atmosphere. The NMR tube was sealed with a septum cap. The sealed sample was removed from the controlled-atmosphere box and cooled to -78 °C. Dioxygen was introduced into the sample through a syringe needle. PFeOOFeP formed after the cold sample was gently shaken. Its formation was monitored by either <sup>1</sup>H NMR or optical spectroscopy. A toluene-*d*<sub>7</sub> solution of *N*-MeIm was added to the sample which was maintained at -70 °C through a microsyringe so that a 2-3 M excess of *N*-MeIm per iron was present. This effected the conversion of PFeOOFeP to (B)PFe<sup>IV</sup>=O. Other spectroscopic handling techniques have been described previously.<sup>27</sup>

**Protein Samples.** HRP, type VI, and sperm whale Mb, type II, were purchased as lyophilized salt-free powders from Sigma and used without further purification. The preparation of apo-HRP and subsequent reconstitution with meso-H-protohemin followed the method of DiNello.<sup>50</sup> Preparation of apo-Mb and reconstitution was by the method of Teale.<sup>51</sup> Protein solutions for NMR study were 2-3 mM in 0.2 M NaCl 99.8% H<sub>2</sub>O. The pH (uncorrected for isotope effect and hence referred to as "pH") was adjusted by addition of microliter amounts of 0.2 M <sup>2</sup>HCl and 0.2 M NaO<sup>2</sup>H. Ferryll Mb was formed<sup>33,52</sup> at pH 7.8 by addition of a 4-fold excess of H<sub>2</sub>O<sub>2</sub> to a solution of the ferric protein in the NMR tube. HRP-II was formed at pH 9.2 by simultaneous addition of 1 equiv each of H<sub>2</sub>O<sub>2</sub> and indole-2-propionic acid<sup>3</sup> (IPA) to a solution of the ferric protein in the NMR tube. The particular pH values were chosen to maximize the stability of the respective ferryll species.

**Spectroscopic Measurements.** <sup>1</sup>H NMR spectra were recorded at 360 MHz on a Nicolet NT-360 FT NMR spectrometer operating in the quadrature mode. For model compds., 300-2000 transients were accumulated over a 10-KHz bandwidth with a 10-μs 90° pulse. Typical protein spectra required 20000-50000 transients collected over a 30-KHz bandwidth. The residual water signal in the protein solutions was suppressed with a 25-μs presaturation pulse, and signal-to-noise was enhanced by exponential apodization which introduced a negligible 20-Hz line broadening. Peak positions (in ppm) for the model compounds were referenced against internal tetramethylsilane, Me<sub>4</sub>Si. For the protein solution, shifts were referenced (in ppm) to the solvent resonance which was in turn calibrated against internal 4,4-dimethyl-4-silapentane-sulfonate, DSS.

Electronic spectra were measured with a Cary 17 spectrophotometer equipped with a Kontes variable-temperature Dewar. The cuvette was cooled by immersion in an ethanol bath which was chilled by the addition of sufficient liquid nitrogen to reach -78 °C.

**Acknowledgment.** We thank the National Institutes of Health (GM-26226, HL-16087, HL-22252) and the National Science Foundation (CHE-81-08766) for support, Professor H. A. Goff for permission to quote his unpublished data given in Table I, and Professor C. A. Reed for a prepublication copy of ref 43. L.L.-G. was on leave from the Institute of Chemistry, University of Wrocław, Poland.

**Registry No.** (Etio)FeOOFe(Etio), 84040-44-8; (OEP)FeOOFe(OEP), 74558-64-8; (*N*-MeIm)(Etio)FeO, 84027-21-4; (*N*-MeIm)(OEP)FeO, 82512-03-6; (*N*-MeIm)(OEP-*meso*-<sup>2</sup>H<sub>4</sub>)FeO, 84027-22-5; peroxidase, 9003-99-0.

(44) Hudson, M. F.; Smith, K. M. *Tetrahedron* **1975**, *31*, 3077-3083.

(45) Fuhrhop, J. H.; Smith, K. M. In "Porphyrins and Metalloporphyrins"; Smith, K. M., Ed.; Elsevier: Amsterdam 1975; pp 816-817.

(46) Kenner, G. W.; Smith, K. M.; Sutton, M. J. *Tetrahedron Lett.* **1973**, 1303-1306.

(47) La Mar, G. N.; Budd, D. L.; Smith, K. M.; Langry, K. C. *J. Am. Chem. Soc.* **1980**, *102*, 1822-1827.

(48) Brault, D.; Rougee, M. *Biochemistry* **1974**, *13*, 4598-4503.

(49) Goff, H.; La Mar, G. N.; Reed, C. A. *J. Am. Chem. Soc.* **1977**, *99*, 3641-3646.

(50) DiNello, R. K. Ph.D. Thesis, Harvard University, 1977.

(51) Teale, F. W. J. *Biochim. Biophys. Acta* **1959**, *25*, 543.

(52) King, N. K.; Winfield, M. E. *J. Biol. Chem.* **1974**, *238*, 1520-1528.